Title

Low Concentrations of Silver Nanoparticles and Silver Ions Perturb the Antioxidant Defense System and Nitrogen Metabolism in N2-Fixing Cyanobacteria

Journal

Environmental Science and Technology, 54(24)

ISSN

0013-936X

Authors

Huang, Min
Keller, Arturo A
Wang, Xiaomi
et al.

Publication Date

2020-12-15

DOI

10.1021/acs.est.0c05300

Peer reviewed

Environmental Science & Technology

pubs.acs.org/est

Article

Low Concentrations of Silver Nanoparticles and Silver Ions Perturb the Antioxidant Defense System and Nitrogen Metabolism in N_2-Fixing Cyanobacteria

Min Huang, Arturo A. Keller, Xiaomi Wang, Liyan Tian, Bing Wu, Rong Ji, and Lijuan Zhao*

Cite This: https://dx.doi.org/10.1021/acs.est.0c05300

Read Online

ACCESS | Metrics & More | Article Recommendations | Supporting Information

ABSTRACT: Although toxic effects of silver nanoparticles (AgNPs) on aquatic organisms have been extensively reported, responses of nitrogen-fixing cyanobacteria to AgNPs/Ag^+ under environmentally relevant concentrations are largely unknown. Here, cyanobacteria were exposed to different concentrations of AgNPs (0.01, 0.1, and 1 mg/L) or Ag^+ (0.1, 1, and 10 μg/L) for 96 h. The impacts of AgNPs and Ag^+ on photosynthesis and N_2 fixation in cyanobacteria (*Nostoc sphaeroides*) were evaluated. In addition, gas chromatography−mass spectrometry (GC−MS)-based metabolomics was employed to give an instantaneous snapshot of the physiological status of the cells under AgNP/Ag^+ exposure. Exposure to high doses of AgNPs (1 mg/L) or Ag^+ (10 μg/L) caused growth inhibition, reactive oxygen species overproduction, malondialdehyde accumulation, and decreased N_2 fixation. In contrast, low doses of AgNPs (0.01 and 0.1 mg/L) and Ag^+ (0.1 and 1 μg/L) did not induce observable responses. However, metabolomics revealed that metabolic reprogramming occurred even at low concentrations of AgNP and Ag^+ exposure. Levels of a number of antioxidant defense-related metabolites, especially phenolic acid and polyphenols (gallic acid, resveratrol, isochlorogenic acid, chlorogenic acid, cinnamic acid, 3-hydroxybenzoic acid, epicatechin, catechin, and ferulic acid), significantly decreased in response to AgNPs or Ag^+. This indicates that AgNPs and Ag^+ can disrupt the antioxidant defense system and disturb nitrogen metabolism even at low-dose exposure. Metabolomics was shown to be a powerful tool to detect "invisible" changes, not observable by typical phenotypic-based endpoints.

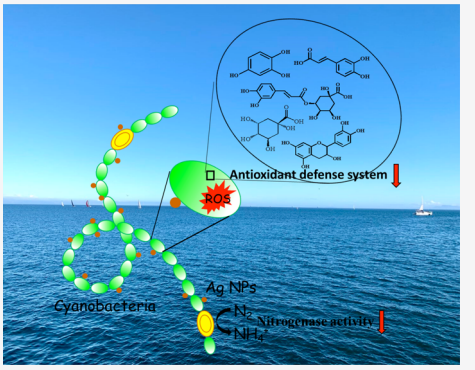

INTRODUCTION

The deployment of nanotechnology has resulted in increasing releases of various engineered nanoparticles (ENPs) into the environment annually.[1] Silver nanoparticles (AgNPs) are by far the most commercialized ENPs in the market due to their excellent antibacterial capacities,[2] and their release and accumulation are expected to increase rapidly. Recently, a few of groups have investigated the environmental concentrations of AgNPs in water bodies. Based on these reports, the observed Ag concentrations in the effluent of wastewater treatment plant (WWTP) and surface water in Switzerland[3,4] and U.S.[5,6] are in a range of 0.04−0.2 μg/L. The predicted environmental concentrations of AgNPs in surface water is even up to 10 μg/L.[7] Due to inadequate elimination of AgNPs by WWTPs, aquatic ecosystems will be a main sink for AgNPs.[8,9]

Understanding the interaction between AgNPs and aquatic organisms, such as algae, cyanobacteria, and fish, is crucial for their environmental assessment. However, the current challenge in studying the toxicological effects of NPs on aquatic organisms is that high exposure doses would generate observable responses, but the real environmental risk can be compromised or misrepresented by the consideration of unrealistic exposure doses.[10] On the other hand, under low exposure doses, the toxic effects are difficult to detect by measuring typical phenotypic-based endpoints, e.g., growth, photosynthesis, and lipid peroxidation.[11] New tools and endpoints are necessary to detect the traditional "invisible" changes in organisms exposed to NPs at environmentally relevant concentrations. Omics are sensitive and powerful tools that can capture molecular changes in organisms holistically.[12] Thus, omics-based endpoints may enable the observation of early molecular changes that provide an early warning on metabolic profile alterations.[13] Among all the omics techniques, metabolomics provides a direct and instantaneous snapshot of the physiological state of the cell, without considering the genetic changes.[14] Under environmental stress conditions, reprogramming of metabolome may occur in the

Received: August 6, 2020
Revised: November 5, 2020
Accepted: November 12, 2020

cell, leading to a targeted metabolic strategy to cope with stress.

Cyanobacteria are ecologically important primary producers in freshwater and marine environments. The photosynthetic impacts of AgNPs on a number of cyanobacteria species (*Synechococcus leopoliensis*,[15] *Synechococcus* sp.,[16] and *Microcystis aeruginosa*[17]) have been investigated. However, certain cyanobacteria species can perform nitrogen fixation and oxygenic photosynthesis simultaneously.[18,19] These nitrogen-fixing cyanobacteria play important roles in both carbon (C) and nitrogen (N) cycling in aquatic ecosystems. Cyanobacteria can also play an important role in supplying nitrogen to non-legume plants, such as maize and rice. Therefore, understanding the impacts of AgNPs on cyanobacteria, especially N_2 fixation and nitrogen metabolism, is of great importance, but few studies have addressed these issues.

The goals of this study were to investigate the response of N_2-fixing cyanobacteria (*Nostoc sphaeroides*) to AgNPs at low concentrations of exposure. Two important biological functions, photosynthesis and N_2 fixation, were evaluated simultaneously. Since AgNPs are known to induce the overproduction of reactive oxygen species (ROS), ROS homeostasis and the antioxidant defense system were also evaluated. In addition, using gas chromatography−mass spectrometry (GC−MS)-based metabolomics, we sought to detect "invisible" metabolic changes at low exposure doses, which may help to understand the mechanisms and underlying processes governing the toxicity of AgNPs to cyanobacteria. The findings of this work will contribute to a thorough, deep, and comprehensive understanding of the environmental implication of AgNPs on cyanobacteria.

EXPERIMENTAL SECTION

AgNP Characterization. AgNPs were purchased from Pantian Nano Material Co., Ltd. (Shanghai, China). The size, shape, and morphology of AgNPs were observed using a transmission electron microscope (TEM) (JEM-200CX, JEOL, Japan). A typical TEM image reveals that the AgNPs are roughly spherical in shape with sizes in the range of 19.9−36.9 nm (Figure S1), with an average of 30.87 nm. The hydrodynamic diameter of AgNPs in ultrapure water, at 100 mg/L, was 134.7 ± 1.38 nm, with a ζ potential of 9.95 ± 0.76 mV, measured via dynamic light scattering (DLS) (Zetasizer Nano ZS, Malvern). A AgNP stock suspension was prepared by adding 1 mg of AgNPs into 100 mL of DI water and sonicated (KH-100DB, Hechuang Ultrasonic, Jiangsu, China) at 45 kHz for 30 min to obtain a well-dispersed suspension.

Cyanobacteria Culture and AgNP Exposure. *Nostoc sphaeroides* cyanobacteria, with an initial density of 1×10^6 *Nostoc* cells mL^{-1}, were obtained from the Institute of Wuhan Hydrobiology, Chinese Academy of Sciences. The growth medium used for the routine culture of *Nostoc* and for AgNP exposure experiments was BG11-N (BG11 without nitrogen, composition in Table S1). *Nostoc* cells were cultured at 25 ± 1 °C with a 12 h/12 h light/dark cycle with a light intensity of 36 μmol photons m^{-2} s^{-1}. Cell optical densities were measured using an optical density at 680 nm (OD 680) with a microplate spectrophotometer (Synergy H4 Hybrid Reader, BioTek, America).

Seven treatments were established, including control (no Ag^+ or AgNPs); 0.01, 0.1, and 1 mg/L AgNPs; and 0.1, 1, and 10 μg/L Ag^+. Previous studies[20,21] and our preliminary experiments showed that approximately 1% of Ag^+ were released from AgNPs over 96 h. These AgNPs and Ag ion concentrations covered a wide range of possible environmentally relevant levels. Among them, the lowest doses of AgNPs (0.01 mg/L) and Ag^+ (0.1 μg/L) are environmentally relevant concentrations according to a previous publication.[7] Each treatment had four replicates. The AgNP stock solutions were prepared immediately prior to exposure experiments. The algal cells were mixed with AgNP or $AgNO_3$ suspensions in 250 mL sterilized flasks and placed in shakers (100 rpm, 25 ± 1 °C) for up to 96 h. The hydrodynamic diameter of AgNPs (100 mg/L) in the growth medium (BG11-N) was 551 ± 17.55 nm, with a ζ potential of 3.8 ± 0.397 mV, measured via DLS.

Morphology of Cyanobacteria Cells. The morphology of cyanobacteria cells and the distribution of AgNPs on the cell surface were observed using a scanning electron microscope (SEM) (FEI Quanta 250 FEG) equipped with an energy-dispersive X-ray spectrometry (EDS) (Oxford Aztec X-MaxN 80 T). Briefly, the samples were fixed in 2.5% glutaraldehyde, dehydrated in gradient concentrations of ethanol, and coated with a layer of gold; then, the images were observed and analyzed for Ag distribution using SEM and EDS.[22]

Transmission electron microscopy (TEM) was employed to observe cell morphology and the distribution of Ag in cyanobacteria cells. Sample preparation for TEM observation was as referenced by Zhang et al.[23] Briefly, cyanobacteria cells treated with AgNPs at 1 mg/L for 96 h were fixed in glutaraldehyde for 4 h followed by staining with osmium tetroxide. After dehydration, embedding, and ultrathin sectioning (60−80 nm), the samples were subsequently observed using TEM (JEM-1200-EX, Japan) with EDS (X-MaxN 80 T, Oxford).

Cell Density and Chlorophyll Content. The optical density of *N. sphaeroides* was monitored using a multimode microplate reader (Synergy H4 Hybrid Reader, BioTek, America) at an absorption wavelength of 680 nm (OD 680). The chlorophyll α measurement was performed according to Sigalat and de Kouchkowski.[24]

Nitrogenase Activity and Total Nitrogen. Nitrogen fixation activity is usually measured by the $^{15}N_2$ stable isotope method or by acetylene reduction assay (ARA).[25] It is believed that $^{15}N_2$ is the most reliable method as this method directly measures N fixation. However, $^{15}N_2$ is costly and requires highly controlled conditions, while the ARA assay is fast and less expensive. Therefore, the nitrogen fixation activities were measured according to the ARA protocol described by Wang et al.[26] The principle of the ARA assay is that the nitrogenase enzyme produces ethylene (C_2H_4) in the presence of acetylene (C_2H_2), so the production of C_2H_4 reflects nitrogenase activity.[25] Specifically, NP−cyanobacteria suspensions were incubated with 10% acetylene in 10 mL serum bottles at 25 °C for 4 h. After incubation, the amount of ethylene in the gas phase was quantified using an Agilent 6850 gas chromatograph equipped with a hydrogen flame ionization detector and an HP-PLOT U column (30 m × 0.32 mm, 10 μm) (Agilent Technologies, La Jolla, CA, U.S.A.). The injection and detector temperatures were 120 and 220 °C, respectively. The column was held at 50 °C for 8 min. The amount of ethylene produced was assessed by measuring the height of the ethylene peak on the chromatogram relative to the length of the reaction. Dilution of pure ethylene was employed to create five-point standard calibration curves ($y = 15.668x + 48.094$, $R^2 = 0.998$).

https://dx.doi.org/10.1021/acs.est.0c05300
Environ. Sci. Technol. XXXX, XXX, XXX−XXX

The detection limit for ethylene was ~2 nmol L^{-1}. Ethylene production occurred linearly over the assay period.

The total nitrogen in cyanobacteria was determined according to the method reported by Studt et al.[27] In the method, the alkaline persulfate reaction oxidizes all nitrogen present in cyanobacteria cells to nitrate, and then nitrate reductase is used to catalyze the reduction of nitrate to nitrite in the presence of nicotinamide adenine dinucleotide. Griess reagents are added to react with nitrate and produce a pink color. The absorbance was measured at 540 nm using a multimode microplate reader (Synergy H4 Hybrid Reader, BioTek, America).

ROS Levels and Lipid Peroxidation in Cyanobacteria Cells. ROS production in cyanobacterial cells was quantified using 2′,7′-dichlorodihydrofluorescein diacetate (H_2DCFDA) as a fluorescence probe.[28] The *Nostoc* cells (1 mL) were incubated with H_2DCFDA (10 μmol/L) at 25 °C for 30 min. The cells were then washed three times with phosphate-buffered saline (PBS) at 0.01 μmol/L and resuspended in 200 μL of PBS. The fluorescence of the molecular probes was detected using a microplate reader (Synergy H4 Hybrid Reader, BioTek, America), with an excitation wavelength of 488 nm and an emission wavelength of 525 nm. Three replicates were performed for each measurement.

The membrane integrity of cyanobacteria cells was evaluated by measuring malondialdehyde (MDA) content, which is the final product of lipid peroxidation. The MDA content was measured by the thiobarbituric acid-reactive substances (TBARS) assay.[29] Specifically, 1 mL of cyanobacteria cells (1×10^5) was mixed with 0.3 mL of 0.1% trichloroacetic acid; the mixture was then centrifuged at 10619 × *g* for 15 min. A 0.2 mL aliquot of the supernatant was mixed with 0.8 mL of 0.5% thiobarbituric acid. After, this the mixture was heated in a water bath at 95 °C for 30 min. After cooling, the UV absorbance was measured at 450, 532, and 600 nm via a microplate reader (Varioskan LUX, Thermo Fisher Scientific, Vantaa, Finland). Lipid peroxidation was expressed as mmol of MDA equivalent per liter of cyanobacteria cells.

GC−MS-Based Cyanobacteria Metabolomics. After exposure to different concentrations of AgNPs or Ag^+ for 96 h, cyanobacteria cells (15 mL) were collected by centrifugation for metabolome analysis. The cell pellets were then washed three times with PBS buffer. Subsequently, the washed cell pellets were immediately frozen in liquid nitrogen for 20 s for complete metabolic inactivation.[30] The frozen samples were stored at −80 °C. The metabolites were extracted from deep-frozen cells using 1 mL of 80% methanol containing a defined amount of the internal standard 2-chloro-L-phenylalanine (0.3 mg/mL) and 200 μL of chloroform. Chloroform is for extracting lipophilic metabolites. The mixtures were sonicated for 30 min followed by centrifugation. The collected supernatant was dried by freeze vacuum drying. The extracted compounds were derivatized using methoxylamine hydrochloride and subsequent *N*,*O*-bis(trimethylsilyl)-trifluoroacetamide. An Agilent 7890B gas chromatograph coupled to an Agilent 5977A mass selective detector (Santa Clara, CA, USA), with a DB-5MS fused silica capillary column (30 m × 0.25 mm internal diameter with 0.25 μm film) (Agilent J&W Scientific, Folsom, CA, USA), was used to run the samples. Quantification was reported as peak height using the unique ion as default. Metabolites were unambiguously assigned by the BinBase identifier numbers using retention index and mass spectrum as the two most important identification criteria. More details regarding sample derivatization and GC−MS analysis are referenced in previous study.[21]

Metabolomics Data Analysis. For GC−MS data, a supervised partial least-squares discriminant analysis (PLS-DA) clustering method was run via online resources (http://www.metaboanalyst.ca/).[31] Before PLS-DA, the data normalization (normalization by sum) was performed for general purpose adjustment based on the differences among samples, and data transformation (log transformation) was conducted to make individual features more comparable. Variable importance in projection (VIP) is the weighted sum of the squares of the PLS-DA analysis, which indicates the importance of a variable to the entire model.[32] A variable with a VIP greater than 1 is regarded as responsible for separation, defined as a discriminating metabolite in this study.[33] Biological pathway analysis was performed based on the GC−MS data using MetaboAnalyst 2.0.[34] The library used in pathway analysis is the *Chlorella variabilis* (green alga) KEGG pathway. The impact value threshold calculated for pathway identification was set at 0.1.[33]

Statistical Analysis. Each treatment was conducted in four replicates. For physiological and biochemical assays, the experimental data are represented as mean ± standard deviation. A one-way ANOVA test was performed followed by Tukey's HSD test using the statistical package SPSS 22.0 (SPSS, Chicago, IL).

RESULTS AND DISCUSSION

***Nostoc* Cyanobacteria Cell Morphology and Localization of AgNPs.** Adsorption and direct contact of NPs with aquatic microorganisms are a prerequisite for toxicity.[35] SEM imaging was used to provide visual identification of the interaction between AgNPs and cyanobacteria. As shown in the SEM images, cyanobacteria cells are arranged in bead-like chains (Figure 1). A typical single cell has a length of 3.26 μm and width of 2.05 μm (Figure 1A). The presence of nanoparticles can be seen on the surface of cyanobacteria exposed to different concentrations of AgNPs (Figure 1B−D). SEM-EDS elemental mapping evidenced that the particles are

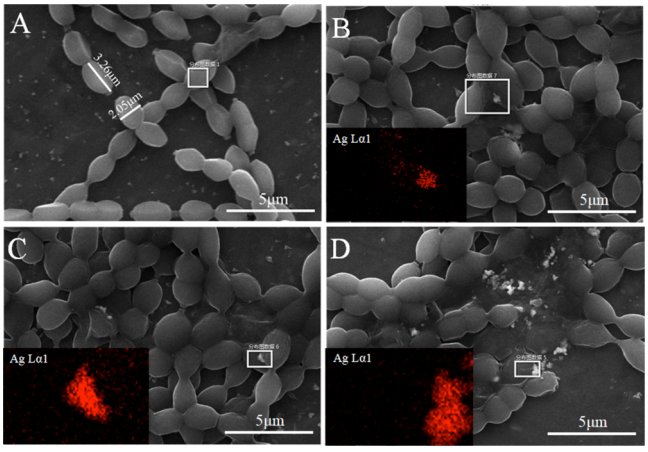

Figure 1. SEM images of cyanobacteria exposed to different concentrations of AgNPs ((A) control without AgNPs, (B) 0.01 mg/L, (C) 0.01 mg/L, and (D) 1 mg/L AgNPs) and SEM-EDS elemental mappings of Ag (red color). Cyanobacteria are cultivated with AgNPs for 96 h at 25 °C with a light intensity of 36 μmol photons m^{-2} s^{-1}.

https://dx.doi.org/10.1021/acs.est.0c05300
Environ. Sci. Technol. XXXX, XXX, XXX−XXX

composed of Ag. It is noteworthy that 0.01 and 0.1 mg/L AgNP exposure did not induce changes in shape, integrity, and morphology of cyanobacteria cells (Figure 1B,C), while 1 mg/L AgNP exposure considerably damaged the integrity of cyanobacteria cells (Figure 1D). The adsorption of NPs onto surfaces of aquatic organisms is governed by multiple factors, such as the physicochemical properties of the NPs and biological substrate (e.g., cell type, cell membrane, and the pathways of cellular processing).[36,37] The forces involved in adsorption of NPs on cells include van der Waals forces, hydrophobic forces, electrostatic attraction, and specific chemical interactions.[38] The positively charged AgNPs (+3.8 mV) likely adhere on the cyanobacteria cell surface through electrostatic attraction. It has been reported that the close particle attachment to the algal cell can result in NP internalization.[23] In addition, Ag ions released from AgNPs might be taken up by cyanobacteria cells. TEM images with elemental analysis (by EDS) further showed the presence of Ag in cyanobacteria cells (Figure S2). However, the information provided by this technique is quite limited. Additional experiments are still needed to clarify that Ag within cells is from Ag ions or from AgNPs.

Effect of AgNPs and Ag^+ on the Growth of Cyanobacteria. After the exposure to different concentrations of AgNPs and Ag^+ for 96 h, cyanobacteria biomass was evaluated via determination of optical density at 680 nm (OD 680). Results showed that the *N. sphaeroides* biomass was unchanged upon exposure to low and medium concentrations of AgNPs (0.01 and 0.1 mg/L) and Ag^+ (0.1 and 1 μg/L) (Figure 2A,B). However, high concentrations of AgNPs and Ag^+ significantly ($p < 0.05$) decreased the cyanobacteria biomass by 25.8 and 10.7%, respectively, compared to the control (Figure 2A,B). Similarly, the chlorophyll content was unchanged upon exposure to low and medium concentrations of AgNPs and Ag^+, while high concentrations of AgNPs and Ag^+ significantly ($p < 0.01$) decreased the chlorophyll content by 32.3 and 18.3%, respectively, compared to the control (Figure 2C,D). In addition, a markedly visible discoloration in cyanobacteria exposed to high concentrations of AgNPs or Ag^+ can be observed (see photographic images of cyanobacteria in Figure 2E,F). These data indicate that AgNPs and Ag^+ at high doses partially inhibited cyanobacteria growth and photosynthesis. These results are not surprising and consistent with previous studies.[39,40] Ag^+ released from AgNPs can result in the formation of oxygen free radicals, which will induce oxidative stress and lead to the inhibited cyanobacteria growth.[41] It is noteworthy that the AgNPs were pristine without surface stabilizing groups. As such, week positive charge may lead to low electrostatic stability and NP agglomeration. The lower surface area will herein likely present slower ionic dissolution and may significantly impact the biological results.

Cyanobacteria Nitrogen Fixation. Since photosynthesis is the principal energy source of adenosine triphosphate for driving nitrogen fixation,[42] we evaluated whether nitrogen fixation activities were impacted by exposure to AgNPs or Ag^+. Nitrogenase activity, reflected by C_2H_4 production, is shown in Figure 3A,B. Nitrogen fixation activity was unchanged upon exposure to low and medium concentrations of AgNPs and Ag^+ but significantly ($p < 0.05$) decreased at high concentrations of AgNPs (94.0%) and Ag^+ (31.0%). Heterocysts are considered the sites of nitrogen fixation by the nitrogenase enzyme. Compared with vegetative cells,

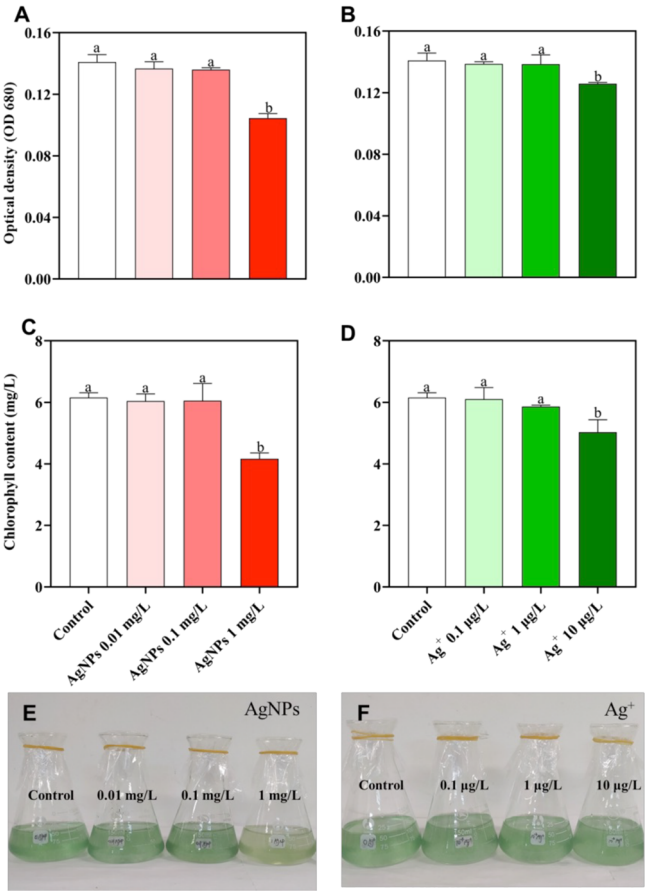

Figure 2. Biomass of cyanobacteria reflected by optical density at 680 nm. Cyanobacteria are exposed to (A) AgNPs and (B) Ag^+. Chlorophyll content of cyanobacteria treated with (C) AgNPs and (D) Ag^+. Visual comparison of cyanobacteria exposed to different concentrations of (E) AgNPs and (F) Ag^+. Cyanobacteria cells are cultivated with AgNPs for 96 h at 25 °C with a light intensity of 36 μmol photons m^{-2} s^{-1}. AgNPs: 0, 0.01, 0.1, and 1 mg/L; Ag^+: 0, 0.1, 1, and 10 μg/L. Error bars represent standard deviations ($n = 4$). Lowercase letters indicate significant differences between treatments.

heterocyst cells have thick-walled modified cells, which help to protect the enzyme nitrogenase from oxygen attack. The decreased N_2 fixation activity may come from either direct disruption of heterocyst's cell membrane or indirectly influenced by the compromised photosynthesis of vegetative cells. To verify if AgNPs and Ag^+ decreased N_2 fixation, the total nitrogen content was determined in cyanobacteria after 96 h of exposure. High concentrations of AgNPs and Ag^+ significantly ($p < 0.05$) decreased the total N content by 23.5 and 6.2%, respectively, in *Nostoc* (Figure 3C,D), which is consistent with the nitrogen fixation activity findings.

Antioxidant System. It has been recognized that AgNPs trigger the overproduction of ROS, which in turn leads to cytotoxicity. The production of ROS in cyanobacteria cells exposed to different concentrations of AgNPs or Ag^+ was determined at 24, 48, 72, and 96 h. Results showed that high doses of AgNP and Ag^+ exposure significantly ($p < 0.05$) increased the ROS level in *Nostoc* cells compared to the control, as early as 24 h, and this tendency persisted until 96 h (Figure 4A). In addition, AgNPs induced more pronounced ROS overproduction, compared to Ag^+, at each time point. These findings are consistent with a previous report that AgNPs and Ag^+ induced overproduction of ROS in algae cells

https://dx.doi.org/10.1021/acs.est.0c05300
Environ. Sci. Technol. XXXX, XXX, XXX−XXX

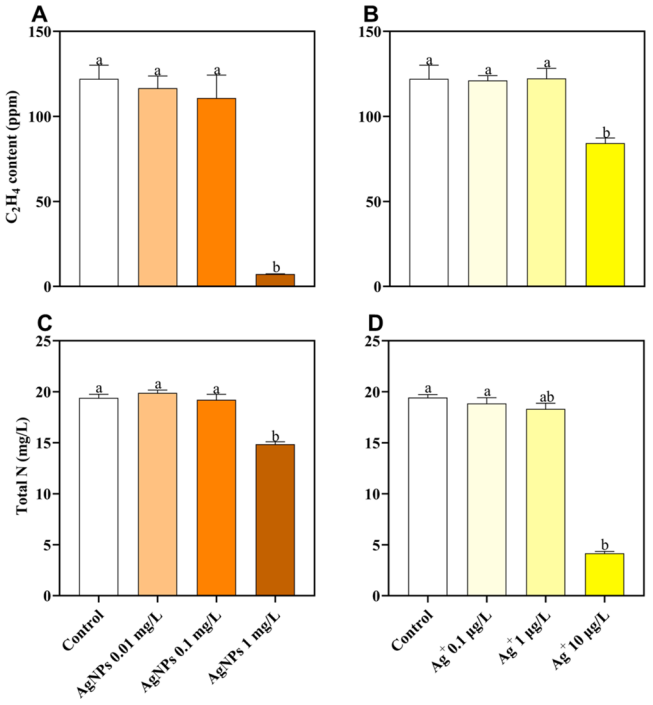

Figure 3. Nitrogenase activity of cyanobacteria treated with (A) AgNPs and (B) Ag^+. Total nitrogen content of cyanobacteria treated with (C) AgNPs and (D) Ag^+. Cyanobacteria cells are cultivated with AgNPs for 96 h at 25 °C with a light intensity of 36 μmol photons m^{-2} s^{-1}. AgNPs: 0, 0.01, 0.1, and 1 mg/L; Ag^+: 0, 0.1, 1, and 10 μg/L. Error bars represent standard deviations (n = 4). Lowercase letters indicate significant differences between treatments.

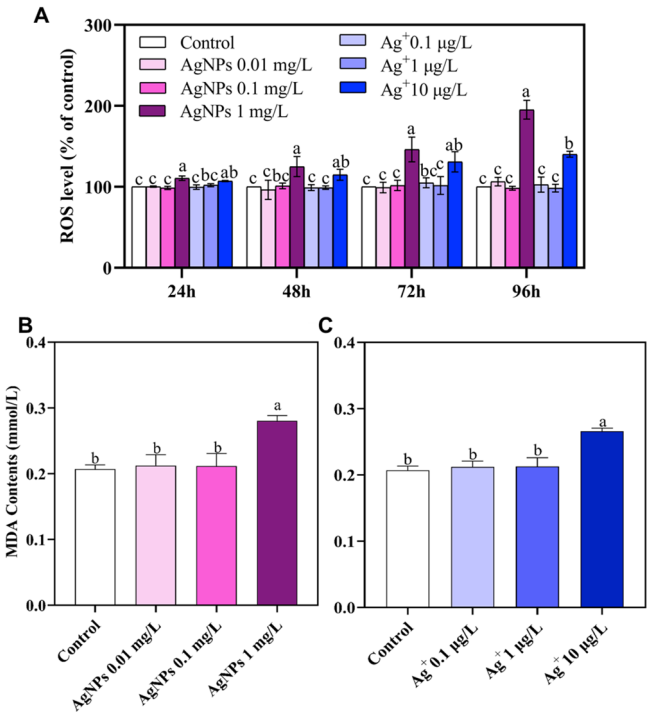

Figure 4. (A) ROS level in cyanobacteria cells after exposure AgNPs or Ag^+ for 24, 48, 72 and 96 h. MDA content of cyanobacteria treated with (B) AgNPs and (C) Ag^+. Cyanobacteria cells are cultivated with AgNPs for 96 h at 25 °C with a light intensity of 36 μmol photons m^{-2} s^{-1}. AgNPs: 0, 0.01, 0.1, and 1 mg/L; Ag^+: 0, 0.1, 1, and 10 μg/L. Error bars represent standard deviations (n = 4). Lowercase letters indicate significant differences between treatments.

(*Chattonella marina*).[43] He et al. also attribute the toxicity of AgNPs to the triggered overproduction of reactive oxygen species.[43]

Lipid membranes are among the most vulnerable cellular components to oxidative stress.[44] MDA, the byproduct of lipid peroxidation, was employed to evaluate whether the overproduced ROS damaged the cell membranes. Results showed that low and medium concentrations of AgNPs and Ag^+ did not change the MDA content in *Nostoc* (Figure 4B,C). However, the MDA content significantly increased upon exposure to high doses of AgNPs (Figure 4B) and Ag^+ (Figure 4C). This indicates that the membrane is the target of ROS-induced attack by AgNPs. Meanwhile, the increased ROS and MDA can explain the growth inhibition after exposure to high doses of AgNPs or Ag^+.

Cell Metabolomics in Response to AgNPs and Ag^+. The above phenotypic- and biochemical-based endpoints reveal that only higher doses of AgNPs (1 mg/L) or Ag^+ (10 μg/L) induced growth inhibition and reduction in nitrogen fixation within 96 h. Using nontargeted GC−MS-based metabolomics, we sought to determine whether metabolomics could reveal some "invisible" changes in cyanobacteria cells exposed to low concentrations of AgNPs or Ag^+, by identifying and quantifying changes in metabolite levels. A total of 193 metabolites were identified and semiquantified. A multivariate analysis, PLS-DA, was conducted to obtain a global view of how the metabolite profile changed. The score plot of the PLS-DA model shows that AgNPs groups are separated from the control group generally in a dose-dependent manner along PC1 (Figure 5A). Similarly, all Ag^+ groups were clearly separated from the control in a dose-dependent way (Figure 5B), as reflected by the score plot. These data indicate that even low and medium concentrations of AgNPs (0.01 and 0.1 mg/L) and Ag^+ (0.1 and 1 μg/L) induced global metabolic reprogramming of intermediates in cyanobacteria; in other words, even low concentrations of AgNPs and Ag^+ disrupted the normal metabolism of cyanobacteria, although there is no observable response at phenotypic and biochemical levels.

To screen out metabolites that differed in concentration between the control and AgNP/Ag^+-exposed groups, univariate analysis (ANOVA and t-test) was performed. Levels of 48 and 102 metabolites were found to be significantly ($p < 0.05$) changed upon exposure to AgNPs and Ag^+ (see the Venn diagram in Figure 5C), respectively, while 39 metabolites overlapped (Figure 5C and Table S2). It is noteworthy that most of the overlapped metabolites are involved in ROS quenching and antioxidant defense. For example, some phenolic acids and polyphenols, including gallic acid, resveratrol, isochlorogenic acid, chlorogenic acid, cinnamic acid, hydroquinone, 3-hydroxybenzoic acid, 1,2,3-trihydroxybenzene, quinic acid, epicatechin, catechin, ferulic acid, and 1,3,5-benzenetriol, decreased in a dose-dependent manner with AgNPs and Ag^+ (see box plots in Figure 6). These phenolic acids are produced in cyanobacteria via shikimic acid through shikimate−phenylpropanoid biosynthesis.[45] Interestingly, two aromatic amino acids (L-tyrosine and phenylalanine), which are precursors for phenolic biosynthesis in the shikimate−phenylpropanoid pathway, increased in a dose-dependent manner after exposure to AgNPs (Figure S3). The underproduction of phenolic acids and overaccumulation of their

https://dx.doi.org/10.1021/acs.est.0c05300
Environ. Sci. Technol. XXXX, XXX, XXX−XXX

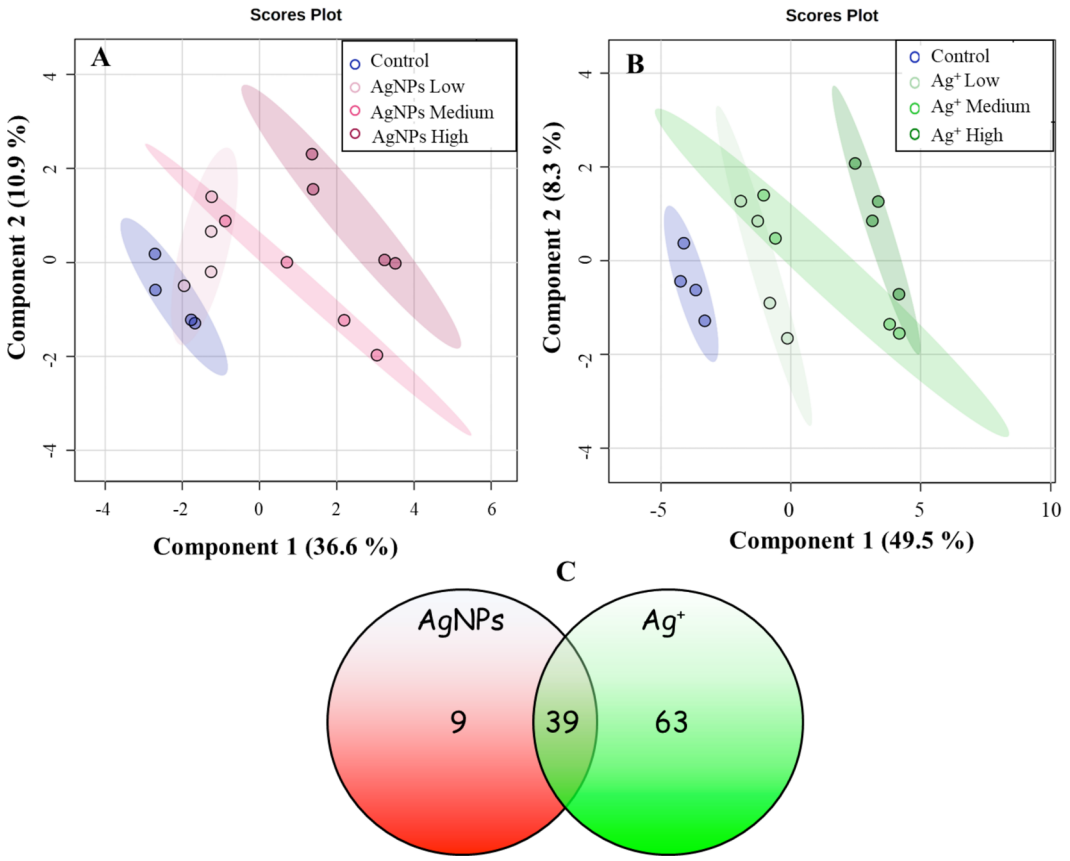

Figure 5. Partial least-squares discriminate analysis (PLS-DA) score plots of metabolic profiles in cyanobacteria treated with (A) AgNPs and (B) Ag^+. (C) Venn diagram of significantly changed metabolites in cyanobacteria treated with AgNPs and Ag^+. AgNPs: 0, 0.01, 0.1, and 1 mg/L; Ag^+: 0, 0.1, 1, and 10 μg/L.

upstream precursors indicate that the overproduced ROS pose detrimental effects on the antioxidant system and defense-related biological pathway of cyanobacteria cells. In addition to phenolic acids or phenolics, more significant changes in levels of metabolites associated with antioxidant defense were observed. For example, AgNPs and Ag^+ caused a significant decrease in oxalic acid (42−64%) in a dose-dependent manner as compared with the control (Figure S4). It has been reported that oxalic acids are able to inhibit the production of H_2O_2 and thus can modulate the oxidative burst of the plant.[46] The downregulation of oxalic acid may indicate a stress defense mechanism in cyanobacteria cells in response to AgNPs. Dehydroascorbic acid (DHA), which is an oxidized form of ascorbic acid (vitamin C), decreased in a dose-dependent manner with AgNP and Ag^+ exposure (Figure S5). DHA is the product of an important antioxidant-associated pathway (ascorbate and aldarate metabolism), acting as a cellular protector against oxidative stress.[47] The consumption of these antioxidant metabolites possibly quenched the overproduction of ROS induced by Ag^+ and prevented the damage to important cellular components. The downregulation of so many antioxidant-related compounds indicates that the antioxidant defense system was activated by AgNPs and Ag^+, even at a low exposure dose. We measured the total antioxidant capacity (TAC) in cyanobacteria cells and found that high concentrations of AgNPs (1 mg/L) and Ag^+ (10 μg/L) significantly ($p < 0.05$) reduced TAC by 15.8 and 10.6%, respectively (Figure S6A,B).

Taken together, the above finding indicates that even low concentrations of AgNPs and Ag^+ compromised or disrupted the antioxidant defense system of cyanobacteria, at levels below those reflected by the determination of ROS and MDA contents. This indicates that MDA, a well-known lipid peroxidation biomarker, does not necessarily provide an early and sensitive warning that the antioxidant system has been disrupted. Since the equilibrium between ROS generation and neutralization was broken, the growth and development of cyanobacteria will be compromised leading even to death after a long-term exposure, although low and medium concentrations of AgNPs and Ag^+ did not induce growth inhibition within 96 h.

Changed Fatty Acids by AgNPs and Ag^+. A noteworthy change is that some saturated fatty acids (palmitelaidic acid, palmitic acid, and lignoceric acid) increase after exposure to low and medium concentrations of AgNPs and Ag^+ but decreased under high doses (Figure S7). The upregulation of saturated fatty acids may indicate a strategy of cyanobacteria to protect the cell from ROS attack by altering the composition of the plasma cell membrane and changing the permeability of the cell membrane. When ROS was overproduced under high AgNP/Ag^+ exposure, the cell membrane was damaged and the level of these fatty acids decreased.

Ag^+ Specific Metabolic Changes. The above discussion addressed metabolic changes that were common to AgNPs and Ag^+, such as decreased antioxidant compounds, increased nitrogen-containing compounds, and perturbed unsaturated fatty acids. The similarities in the metabolic reprogramming

https://dx.doi.org/10.1021/acs.est.0c05300
Environ. Sci. Technol. XXXX, XXX, XXX−XXX

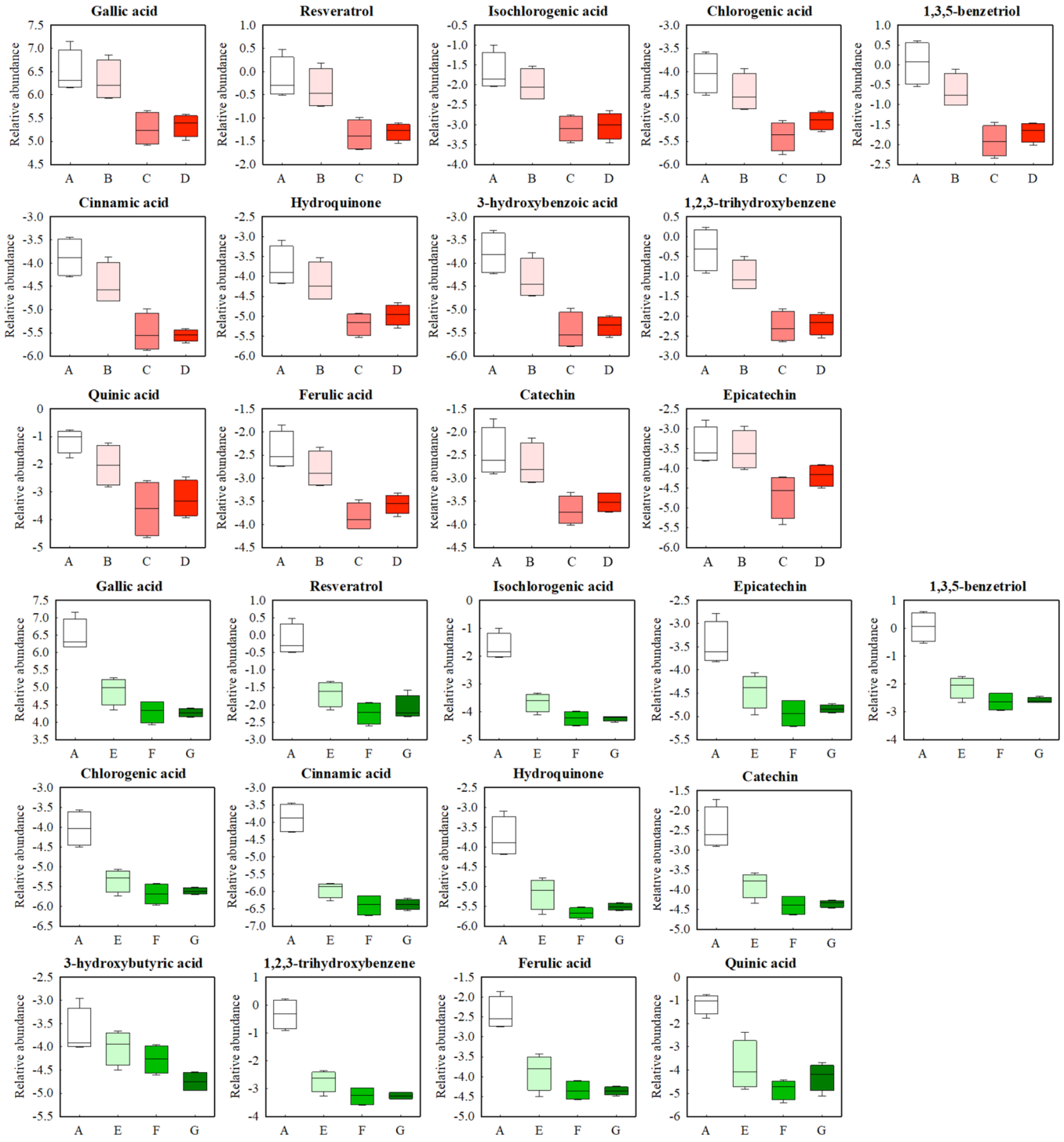

Figure 6. Box plots of relative abundance of antioxidant metabolites in cyanobacteria exposed to different doses of AgNPs and Ag^+ (n = 4). (A–D) 0, 0.01, 0.1, and 1 mg/L AgNPs, respectively. (E–G) 0.1, 1, and 10 μg/L Ag^+, respectively. The scales of relative abundance in box plots are given in logarithmic values.

pattern suggest that parts of the responses in cyanobacteria induced by AgNPs are due to the dissolved Ag ions. However, it cannot be neglected that Ag^+ induced a much stronger metabolic response compared to AgNPs. As can be seen in Figure S8, levels of additional antioxidant-related metabolites (pelargonic acid, protocatechuic acid, and α-tocopherol, and 1,2,4-benzenetriol) were decreased by Ag^+, compared to AgNPs (Figure 6). Furthermore, unlike AgNP exposure, which gradually decreased antioxidants with increasing AgNP exposure concentration (see box plots in Figure 6), Ag^+ even at the lowest dose induced a marked decrease in antioxidant levels (Figure S8). In addition, glutathione (GSH) was unchanged under AgNP exposure but significantly increased in response to Ag^+ (Figure S9). GSH not only acts as a signaling molecule but also plays an important role in protecting macromolecules against attack by eliminating free radicals, which are formed as a consequence of oxidative stress.[48] GSH might be the second line of antioxidant defense,

https://dx.doi.org/10.1021/acs.est.0c05300
Environ. Sci. Technol. XXXX, XXX, XXX–XXX

compared to phenolics. This indicates that Ag^+ induced more pronounced negative effects on the antioxidant defense system. Taylor et al.[15] also found that ionic silver had more negative effects, compared to AgNPs, on the toxic stress endpoints. This may reflect the slow release dynamics of Ag^+ from AgNPs, compared to Ag^+ from $AgNO_3$, which is almost immediately available.

Additionally, levels of a number of metabolites, which were unchanged by exposure to AgNPs, were increased by Ag^+ treatment, such as ethylamine, nicotinic acid, inositol-4-monophosphate, urea, malic acid, serine, glycine, norvaline, thymine, lysine, glutamic acid, aspartic acid, threonine, ribose, D-fructose-6-phosphate, and glucose-6-phosphate. Again, this indicates that Ag^+ induced a stronger response to the oxidative stress and more pronounced metabolic reprogramming, compared to AgNPs. Possibly, the upregulation of these compounds is the strategy cyanobacteria employed to cope with the disrupted ROS homeostasis. In Figure S10, six amino acids (glycine, serine, L-threonine, L-aspartic acid, L-glutamic acid, and thymine), one organic acid (malic acid), and two sugars (D-fructose-6-phosphate and glucose-6-phosphate) share very similar metabolic change patterns under Ag^+ treatment. Levels of these metabolites increased in a dose-dependent manner from control to low and medium doses, but then either did not increase or even declined at high concentrations of Ag^+ exposure. We speculate that cyanobacteria cells actively reprogram the metabolome to cope with the stress before Ag^+ reaches the threshold. The changes of these carbohydrates and amino acids are indicative of perturbations to carbon and nitrogen metabolism.

Metabolic pathway analysis reveals that AgNPs at a low concentration (0.01 mg/L) did not induce any pathway perturbation (Table S3), while even the lowest dose of Ag^+ (0.1 μg/L) induced perturbation of nine biological pathways, including β-alanine metabolism; glyoxylate and dicarboxylate metabolism; arginine biosynthesis; cysteine and methionine metabolism; pantothenate and coenzyme A biosynthesis; glycine, serine, and threonine metabolism; arginine and proline metabolism; isoquinoline alkaloid biosynthesis; and tyrosine metabolism (Table S3). Medium and high concentrations of Ag^+ induced perturbations in 14 and 21 biological pathways, respectively (Table S3). In contrast, medium and high concentrations of AgNPs induced only 10 and 12 metabolic pathway perturbations, respectively. Therefore, pathway analysis confirmed that Ag^+ induced more pronounced metabolic changes compared to AgNPs. Most of the pathways perturbed by AgNPs and Ag^+ were related to nitrogen metabolism, as indicated by the nitrogen assays. Carbon metabolism is linked to the incomplete tricarboxylic acid cycle in cyanobacteria cells; perturbations to a number of carbon-related metabolic pathways were observed, such as glyoxylate and dicarboxylate metabolism and starch and sucrose metabolism. Taken together, although low concentrations of AgNPs and Ag^+ did not impact N_2 fixation, carbon and nitrogen metabolism was perturbed.

Environmental Implication. In this study, we systematically investigated the impact of AgNPs on N_2-fixing cyanobacteria (*N. sphaeroides*) during short-term exposure (96 h); these cyanobacteria are important components of many ecosystems. In addition to considering typical phenotypic- and biochemical-based endpoints (OD 680, chlorophyll, ROS, and MDA) to evaluate the impact of AgNPs on cyanobacteria, we also evaluated the metabolic responses of *Nostoc* cyanobacteria to AgNPs and Ag^+ via GC–MS-based metabolomics. While only high doses of AgNPs and Ag^+ induced physiological responses (growth inhibition, overproduction of ROS, increased MDA, and decreased N_2 fixation), indicating the imbalance of ROS homeostasis and oxidative stress, metabolomics revealed that even low doses of AgNPs and Ag^+ induced metabolite profile alterations in *N. sphaeroides*. Levels of a number of antioxidant-related metabolites, especially phenolics, markedly decreased upon exposure to either AgNPs or Ag^+, even at low doses, indicating a perturbed antioxidant defense system. Since cyanobacteria play an important role in C and N cycling in ecosystems, the perturbed antioxidant system and nitrogen metabolism by AgNPs and Ag^+ will indirectly influence C and N cycling in aquatic or terrestrial ecosystems. In this study, the lowest concentration of Ag^+ (0.1 μg/L) evaluated falls within the range of observed environmental concentrations (0.04–0.2 μg/L). We demonstrate that even at such a low dose, Ag^+ can perturb the metabolism in cyanobacteria, disrupting the antioxidant defense system. Small molecules are markedly regulated by upstream gene expression and transcript formation; thus, changes in gene expression must have occurred even at low doses of Ag^+. Metabolomics can serve to detect these "invisible" changes. The physiological changes, which typical endpoints cannot detected, may be captured by metabolomics.

■ ASSOCIATED CONTENT

Supporting Information

The Supporting Information is available free of charge at https://pubs.acs.org/doi/10.1021/acs.est.0c05300.

Composition of BG11-N (Table S1); metabolites significantly changed in cyanobacteria exposed to AgNPs or Ag^+ (Table S2); perturbed metabolic pathways in cyanobacteria cells by AgNPs (0, 0.01, 0.1, and 1 mg/L) and Ag^+ (0, 0.1, 1, 10 μg/L) exposure (Table S3); TEM image of AgNPs (Figure S1); TEM images of the *Nostoc* cells with elemental analysis (EDS) showing the presence of Ag within cells (Figure S2); box plots of L-tyrosine and phenylalanine levels in cyanobacteria cells (Figure S3); box plots of relative abundance of oxalic acid in cyanobacteria treated with different doses of AgNPs and Ag^+ (Figure S4); box plots of DHA levels in cyanobacteria cells (Figure S5); TAC of cyanobacteria cells (Figure S6); box plots of saturated fatty acids in cyanobacteria cells with AgNP and Ag^+ exposure (Figure S7); box plots of antioxidant-related metabolites exposed to Ag^+ (Figure S8); box plots of GSH levels in cyanobacteria cells with AgNP and Ag^+ exposure (Figure S9); and box plots of six amino acids, one organic acids, and two sugars exposed to Ag^+ (Figure S10) (PDF)

■ AUTHOR INFORMATION

Corresponding Author

Lijuan Zhao − *State Key Laboratory of Pollution Control and Resource Reuse, School of Environment, Nanjing University, Nanjing 210023, China;* orcid.org/0000-0002-8481-0435; Phone: +86 025-8968 0581; Email: ljzhao@nju.edu.cn; Fax: +86 025-8968 0581

https://dx.doi.org/10.1021/acs.est.0c05300
Environ. Sci. Technol. XXXX, XXX, XXX−XXX

Authors

Min Huang − *State Key Laboratory of Pollution Control and Resource Reuse, School of Environment, Nanjing University, Nanjing 210023, China*

Arturo A. Keller − *Bren School of Environmental Science & Management and Center for Environmental Implications of Nanotechnology, University of California, Santa Barbara, California 93106, United States;* orcid.org/0000-0002-7638-662X

Xiaomi Wang − *Key Laboratory of Soil Environment and Pollution Remediation, Institute of Soil Science, Chinese Academy of Sciences, Nanjing 210008, China*

Liyan Tian − *State Key Laboratory of Pollution Control and Resource Reuse, School of Environment, Nanjing University, Nanjing 210023, China*

Bing Wu − *State Key Laboratory of Pollution Control and Resource Reuse, School of Environment, Nanjing University, Nanjing 210023, China;* orcid.org/0000-0001-7117-580X

Rong Ji − *State Key Laboratory of Pollution Control and Resource Reuse, School of Environment, Nanjing University, Nanjing 210023, China;* orcid.org/0000-0002-1724-5253

Complete contact information is available at: https://pubs.acs.org/10.1021/acs.est.0c05300

Notes

The authors declare no competing financial interest.

■ ACKNOWLEDGMENTS

This work was funded by the National Natural Science Foundation of China under 21876081 and 21906081. A.A.K. was funded by the United States National Science Foundation under 1901515. Any opinions, findings, conclusions, or recommendations expressed in this material are those of authors and do not necessarily reflect the views of the National Science Foundation of China or the United States National Science Foundation.

■ REFERENCES

(1) Keller, A. A.; Lazareva, A. Predicted Releases of Engineered Nanomaterials: From Global to Regional to Local. *Environ. Sci. Technol. Lett.* **2013**, *1*, 65−70.

(2) Flores-López, L. Z.; Espinoza-Gómez, H.; Somanathan, R. Silver nanoparticles: Electron transfer, reactive oxygen species, oxidative stress, beneficial and toxicological effects. *Mini Rev.* **2019**, *39*, 16−26.

(3) Mueller, N. C.; Nowack, B. Exposure Modeling of Engineered Nanoparticles in the Environment. *Environ. Sci. Technol.* **2008**, *42*, 4447−4453.

(4) Gottschalk, F.; Sonderer, T.; Scholz, R. W.; Nowack, B. Modeled Environmental Concentrations of Engineered Nanomaterials (TiO2, ZnO, Ag, CNT, Fullerenes) for Different Regions. *Environ. Sci. Technol.* **2009**, *43*, 9216−9222.

(5) Mitrano, D. M.; Lesher, E. K.; Bednar, A.; Monserud, J.; Higgins, C. P.; Ranville, J. F. Detecting nanoparticulate silver using single-particle inductively coupled plasma−mass spectrometry. *Environ. Toxicol. Chem.* **2012**, *31*, 115−121.

(6) Cervantes-Avilés, P.; Huang, Y.; Keller, A. A. Incidence and persistence of silver nanoparticles throughout the wastewater treatment process. *Water Res.* **2019**, *156*, 188−198.

(7) Maurer-Jones, M. A.; Gunsolus, I. L.; Murphy, C. J.; Haynes, C. L. Toxicity of Engineered Nanoparticles in the Environment. *Anal. Chem.* **2013**, *85*, 3036−3049.

(8) Kaegi, R.; Voegelin, A.; Ort, C.; Sinnet, B.; Thalmann, B.; Krismer, J.; Hagendorfer, H.; Elumelu, M.; Mueller, E. Fate and transformation of silver nanoparticles in urban wastewater systems. *Water Res.* **2013**, *47*, 3866−3877.

(9) Lazareva, A.; Keller, A. A. Estimating Potential Life Cycle Releases of Engineered Nanomaterials from Wastewater Treatment Plants. *ACS Sustainable Chem. Eng.* **2014**, *2*, 1656−1665.

(10) Liu, S.; Lu, Y.; Chen, W. Bridge knowledge gaps in environmental health and safety for sustainable development of nano-industries. *Nano Today* **2018**, *23*, 11−15.

(11) Holden, P. A.; Gardea-Torresdey, J. L.; Klaessig, F.; Turco, R. F.; Mortimer, M.; Hund-Rinke, K.; Cohen Hubal, E. A.; Avery, D.; Barceló, D.; Behra, R.; Cohen, Y.; Deydier-Stephan, L.; Ferguson, P. L.; Fernandes, T. F.; Herr Harthorn, B.; Henderson, W. M.; Hoke, R. A.; Hristozov, D.; Johnston, J. M.; Kane, A. B.; Kapustka, L.; Keller, A. A.; Lenihan, H. S.; Lovell, W.; Murphy, C. J.; Nisbet, R. M.; Petersen, E. J.; Salinas, E. R.; Scheringer, M.; Sharma, M.; Speed, D. E.; Sultan, Y.; Westerhoff, P.; White, J. C.; Wiesner, M. R.; Wong, E. M.; Xing, B.; Steele Horan, M.; Godwin, H. A.; Nel, A. E. Considerations of Environmentally Relevant Test Conditions for Improved Evaluation of Ecological Hazards of Engineered Nanomaterials. *Environ. Sci. Technol.* **2016**, *50*, 6124−6145.

(12) Majumdar, S.; Keller, A. A. Omics to address the opportunities and challenges of nanotechnology in agriculture. *Crit. Rev. Environ. Sci. Technol.* **2020**, 1−42.

(13) Buesen, R.; Chorley, B. N.; da Silva Lima, B.; Daston, G.; Deferme, L.; Ebbels, T.; Gant, T. W.; Goetz, A.; Greally, J.; Gribaldo, L.; Hackermüller, J.; Hubesch, B.; Jennen, D.; Johnson, K.; Kanno, J.; Kauffmann, H.-M.; Laffont, M.; McMullen, P.; Meehan, R.; Pemberton, M.; Perdichizzi, S.; Piersma, A. H.; Sauer, U. G.; Schmidt, K.; Seitz, H.; Sumida, K.; Tollefsen, K. E.; Tong, W.; Tralau, T.; van Ravenzwaay, B.; Weber, R. J. M.; Worth, A.; Yauk, C.; Poole, A. Applying 'omics technologies in chemicals risk assessment: Report of an ECETOC workshop. *Regul. Toxicol. Pharmacol.* **2017**, *91*, S3−S13.

(14) Kumar, R.; Bohra, A.; Pandey, A. K.; Pandey, M. K.; Kumar, A. Metabolomics for Plant Improvement: Status and Prospects. *Front. Plant Sci.* **2017**, *8*, 1302.

(15) Taylor, C.; Matzke, M.; Kroll, A.; Read, D. S.; Svendsen, C.; Crossley, A. Toxic interactions of different silver forms with freshwater green algae and cyanobacteria and their effects on mechanistic endpoints and the production of extracellular polymeric substances. *Environ. Sci.: Nano* **2016**, *3*, 396−408.

(16) Burchardt, A. D.; Carvalho, R. N.; Valente, A.; Nativo, P.; Gilliland, D.; Garcìa, C. P.; Passarella, R.; Pedroni, V.; Rossi, F.; Lettieri, T. Effects of Silver Nanoparticles in Diatom Thalassiosira pseudonana and Cyanobacterium Synechococcus sp. *Environ. Sci. Technol.* **2012**, *46*, 11336−11344.

(17) Qian, H.; Zhu, K.; Lu, H.; Lavoie, M.; Chen, S.; Zhou, Z.; Deng, Z.; Chen, J.; Fu, Z. Contrasting silver nanoparticle toxicity and detoxification strategies in Microcystis aeruginosa and Chlorella vulgaris: New insights from proteomic and physiological analyses. *Sci. Total Environ.* **2016**, *572*, 1213−1221.

(18) Singh, J. S.; Kumar, A.; Rai, A. N.; Singh, D. P. Cyanobacteria: A Precious Bio-resource in Agriculture, Ecosystem, and Environmental Sustainability. *Front. microbiol.* **2016**, *7*, 529−529.

(19) Rai, A. N.; Singh, A. K.; Syiem, M. B. Chapter 23 - Plant Growth-Promoting Abilities in Cyanobacteria. In *Cyanobacteria*; Mishra, A. K.; Tiwari, D. N.; Rai, A. N., Eds. Academic Press: 2019; pp. 459−476.

(20) Wang, J.; Koo, Y.; Alexander, A.; Yang, Y.; Westerhof, S.; Zhang, Q.; Schnoor, J. L.; Colvin, V. L.; Braam, J.; Alvarez, P. J. J. Phytostimulation of Poplars and Arabidopsis Exposed to Silver Nanoparticles and Ag+ at Sublethal Concentrations. *Environ. Sci. Technol.* **2013**, *47*, 5442−5449.

(21) Zhang, H.; Du, W.; Peralta-Videa, J. R.; Gardea-Torresdey, J. L.; White, J. C.; Keller, A.; Guo, H.; Ji, R.; Zhao, L. Metabolomics Reveals How Cucumber (Cucumis sativus) Reprograms Metabolites To Cope with Silver Ions and Silver Nanoparticle-Induced Oxidative Stress. *Environ. Sci. Technol.* **2018**, *52*, 8016−8026.

(22) Wu, D.; Yang, S.; Du, W.; Yin, Y.; Zhang, J.; Guo, H. Effects of titanium dioxide nanoparticles on Microcystis aeruginosa and microcystins production and release. *J. Hazard. Mater.* **2019**, *377*, 1−7.
(23) Zhang, L.; Lei, C.; Yang, K.; White, J. C.; Lin, D. Cellular response of Chlorella pyrenoidosa to oxidized multi-walled carbon nanotubes. *Environ. Sci.: Nano* **2018**, *5*, 2415−2425.
(24) Sigalat, C.; de Kouchkowski, Y. Fractionnement et caracterisation de l'algue bleue unicellulaire Anacystis nidulans. *Physiol. Veg.* **1975**, *13*, 243−258.
(25) Belnap, J. Nitrogen fixation in biological soil crusts from southeast Utah, USA. *Biol. Fertil. Soils* **2002**, *35*, 128−135.
(26) Wang, X.; Teng, Y.; Tu, C.; Luo, Y.; Greening, C.; Zhang, N.; Dai, S.; Ren, W.; Zhao, L.; Li, Z. Coupling between Nitrogen Fixation and Tetrachlorobiphenyl Dechlorination in a Rhizobium−Legume Symbiosis. *Environ. Sci. Technol.* **2018**, *52*, 2217−2224.
(27) Studt, J. L.; Campbell, E. R.; Westrick, D.; Kinnunen-Skidmore, T.; Marceau, A. H.; Campbell, W. H. Non-toxic total nitrogen determination using a low alkaline persulfate digestion. *MethodsX* **2020**, *7*, 100791.
(28) Zhang, M.; Wang, H.; Liu, P.; Song, Y.; Huang, H.; Shao, M.; Liu, Y.; Li, H.; Kang, Z. Biotoxicity of degradable carbon dots towards microalgae Chlorella vulgaris. *Environ. Sci.: Nano* **2019**, *6*, 3316−3323.
(29) Jambunathan, N. Determination and Detection of Reactive Oxygen Species (ROS), Lipid Peroxidation, and Electrolyte Leakage in Plants. In *Plant Stress Tolerance: Methods and Protocols*; Sunkar, R., Ed. Humana Press: Totowa, NJ, 2010; pp. 291−297.
(30) Schwarz, D.; Nodop, A.; Hüge, J.; Purfürst, S.; Forchhammer, K.; Michel, K.-P.; Bauwe, H.; Kopka, J.; Hagemann, M. Metabolic and Transcriptomic Phenotyping of Inorganic Carbon Acclimation in the Cyanobacterium Synechococcus elongatus PCC 7942. *Plant Physiol.* **2011**, *155*, 1640−1655.
(31) Xia, J.; Sinelnikov, I. V.; Han, B.; Wishart, D. S. MetaboAnalyst 3.0—making metabolomics more meaningful. *Nucleic Acids Res.* **2015**, *43*, W251−W257.
(32) Jung, Y.; Ahn, Y. G.; Kim, H. K.; Moon, B. C.; Lee, A. Y.; Ryu, D. H.; Hwang, G.-S. Characterization of dandelion species using 1H NMR-and GC-MS-based metabolite profiling. *Analyst* **2011**, *136*, 4222−4231.
(33) Xia, J.; Wishart, D. S. MSEA: a web-based tool to identify biologically meaningful patterns in quantitative metabolomic data. *Nucleic Acids Res.* **2010**, *38*, W71−W77.
(34) Jarvie, H. P.; Al-Obaidi, H.; King, S. M.; Bowes, M. J.; Lawrence, M. J.; Drake, A. F.; Green, M. A.; Dobson, P. J. Fate of silica nanoparticles in simulated primary wastewater treatment. *Environ. Sci. Technol.* **2009**, *43*, 8622.
(35) Batley, G. E.; Kirby, J. K.; McLaughlin, M. J. Fate and Risks of Nanomaterials in Aquatic and Terrestrial Environments. *Acc. Chem. Res.* **2013**, *46*, 854−862.
(36) von Moos, N.; Bowen, P.; Slaveykova, V. I. Bioavailability of inorganic nanoparticles to planktonic bacteria and aquatic microalgae in freshwater. *Environ. Sci.: Nano* **2014**, *1*, 214−232.
(37) Handy, R. D.; Owen, R.; Valsami-Jones, E. The ecotoxicology of nanoparticles and nanomaterials: current status, knowledge gaps, challenges, and future needs. *Ecotoxicology* **2008**, *17*, 315−325.
(38) Ma, S.; Lin, D. The biophysicochemical interactions at the interfaces between nanoparticles and aquatic organisms: adsorption and internalization. *Environ. Sci.: Processes Impacts* **2013**, *15*, 145−160.
(39) Duong, T. T.; Le, T. S.; Tran, T. T. H.; Nguyen, T. K.; Ho, C. T.; Dao, T. H.; Le, T. P. Q.; Nguyen, H. C.; Dang, D. K.; Le, T. T. H.; Ha, P. T. Inhibition effect of engineered silver nanoparticles to bloom forming cyanobacteria. *Adv. Nat. Sci.: Nanosci. Nanotechnol.* **2016**, *7*, No. 035018.
(40) Köser, J.; Engelke, M.; Hoppe, M.; Nogowski, A.; Filser, J.; Thöming, J. Predictability of silver nanoparticle speciation and toxicity in ecotoxicological media. *Environ. Sci.: Nano* **2017**, *4*, 1470−1483.
(41) Nel, A.; Xia, T.; Mädler, L.; Li, N. Toxic Potential of Materials at the Nanolevel. *Science* **2006**, *311*, 622−627.
(42) Alberte, R. S.; Tel-Or, E.; Packer, L.; Thornber, J. P. Functional organisation of the photo-synthetic apparatus in heterocysts of nitrogen-fixing cyanobacteria. *Nature* **1980**, *284*, 481−483.
(43) He, D.; Dorantes-Aranda, J. J.; Waite, T. D. Silver Nanoparticle—Algae Interactions: Oxidative Dissolution, Reactive Oxygen Species Generation and Synergistic Toxic Effects. *Environ. Sci. Technol.* **2012**, *46*, 8731−8738.
(44) Axelsen, P. H.; Komatsu, H.; Murray, I. V. J. Oxidative Stress and Cell Membranes in the Pathogenesis of Alzheimer's Disease. *Physiology* **2011**, *26*, 54−69.
(45) Mandal, S. M.; Chakraborty, D.; Dey, S. Phenolic acids act as signaling molecules in plant-microbe symbioses. *Plant signaling behav.* **2010**, *5*, 359−368.
(46) Cessna, S. G.; Sears, V. E.; Dickman, M. B.; Low, P. S. Oxalic Acid, a Pathogenicity Factor for Sclerotinia sclerotiorum, Suppresses the Oxidative Burst of the Host Plant. *Plant cell* **2000**, *12*, 2191−2199.
(47) Kim, E. J.; Park, Y. G.; Baik, E. J.; Jung, S. J.; Won, R.; Nahm, T. S.; Lee, B. H. Dehydroascorbic acid prevents oxidative cell death through a glutathione pathway in primary astrocytes. *J. Neurosci. Res.* **2005**, *79*, 670−679.
(48) Dubreuil, C.; Poinssot, B. Role of glutathione in plant signaling under biotic stress. *Plant signaling behav.* **2012**, *7*, 210−212.

https://dx.doi.org/10.1021/acs.est.0c05300
Environ. Sci. Technol. XXXX, XXX, XXX−XXX